Compaction of Ribosomal Protein S6 by Sucrose Occurs Only Under Native Conditions†

LuYang Chen,‡ José A. B. Ferreira,§ Sílvia M. B. Costa,§ Gonçalo J. M. Cabrita,‡ Daniel E. Otzen,|| and Eduardo Pinho Melo*,‡,⊥

Centro de Engenharia Biológica e Química, Instituto Superior Técnico, Av. Rovisco Pais 1049-001, Lisboa, Portugal, Centro de Química Estrutural, Instituto Superior Técnico, Av. Rovisco Pais 1049-001, Lisboa, Portugal, Department of Life Sciences, Aalborg University, Sohngaardsholmsvej 49, DK-9000 Aalborg, Denmark, and Centro de Biomedicina Molecular e Estrutural, Universidade do Algarve, Campus de Gambelas, 8005-138 Faro, Portugal

Received July 27, 2005; Revised Manuscript Received November 29, 2005

ABSTRACT: The effect of osmolyte sucrose on the stability and compaction of the folded and unfolded states of ribosomal protein S6 from *Thermus thermophilus* was analyzed. Confirming previous results obtained with sodium sulfate and trehalose, refolding stopped-flow measurements of S6 show that sucrose favors the conversion of the unfolded state ensemble to a highly compact structure (75% as compact as the folded state). This conversion occurs when the unfolded state is suddenly placed under native conditions and the compact state accumulates in a transient off-folding pathway. This effect of sucrose on the compaction of the unfolded state ensemble is counteracted by guanidinium hydrochloride. The compact state does not accumulate at higher guanidinium concentrations and the unfolded state ensemble does not display increased compaction in the presence of 6 M guanidinium as evaluated by collisional quenching of tryptophan fluorescence. In contrast, accessibility of the tryptophan residue of folded S6 above 1 M sucrose concentration decreased as a result of an increased compaction of the folded state. Unfolding stopped-flow measurements of S6 reflect this increased compaction of the folded state, but the unfolding pathway is not affected by sucrose. Compaction of folded and unfolded S6 induced by sucrose occurs under native conditions indicating that decreased protein conformational entropy significantly contributes to the mechanism of protein stabilization by osmolytes.

Compatible solutes, also known as osmolytes, accumulate intracellulary in response to stress conditions such as high temperature and salinity to protect cell structure and function. Proteins are stabilized, DNA conformation and transcription is affected, and membrane order, fluidity, and transition characteristics also change in the presence of osmolytes (*1*, *2*). Several compounds have been identified as cell compatible osmolytes. They are water-soluble compounds of relatively low molecular mass, rarely larger than disaccharides, and they can be classified as nitrogenous compounds (for instance, glutamate, proline, ectoine, and glycine betaine), polyols (glycerol), and carbohydrates (sucrose, fructose, and trehalose, among others).

The effect of osmolytes on protein stability in vitro has been extensively characterized, and some key concepts have emerged. These compounds are preferentially excluded from the surface of the protein, at least around room temperature, leading to an increase of the chemical potential of the protein (*3*−*5*). The Wyman linkage relationship expresses quantitatively the effect of this preferential exclusion on the equilibrium constant of unfolding. It states that upon a change in the osmolyte concentration the change in the equilibrium constant is given by the difference in the number of osmolyte molecules bound by the unfolded and folded protein molecules. Because the preferential exclusion (decreased binding) is larger for the unfolded state because it has more solvent-exposed surface area than that of the folded state, the increase in chemical potential is greater for the unfolded state, which then is destabilized relative to the folded state. The reason for preferential exclusion was attributed to the unfavorable interaction between the peptide backbone and the osmolyte, as the side chains collectively favor interactions with osmolytes (*6*−*8*).

This conceptual framework explaining protein stabilization by osmolytes is, however, simplistic because it neglects any effect of the osmolyte on protein structure. Interactions at the level of secondary and tertiary structure are determinants of protein stability not only for folded but also for unfolded states, as suggested recently(*9*). Therefore, it is important to know what the consequences are of the preferential exclusion phenomena at the level of protein structure and if this somehow affects protein stability. To date, the effect of osmolytes on protein structure is still poorly characterized. Some reports have shown that osmolytes induce the acquisition of protein structure. Denaturated carboxamidated ribonuclease A was shown to contract in the presence of the

† L.Y.C. acknowledges a Ph.D. fellowship (contract SFRH/BD/2821/2000) from Fundação para a Ciência e Tecnologia, Portugal.

* To whom correspondence should be addressed. Phone: 351218419137. Fax: 351218419062. E-mail: emelo@ualg.pt.

‡ Centro de Engenharia Biológica e Química, Instituto Superior Técnico.

§ Centro de Química Estrutural, Instituto Superior Técnico.

|| Aalborg University.

⊥ Universidade do Algarve.

10.1021/bi051490g CCC: $33.50
Published on Web 01/31/2006

osmolytes trimethylamine *N*-oxide, sarcosine, sucrose, and proline (*10*). Acid-denaturated chymotrypsin inhibitor 2 acquires a non-native secondary structure in the presence of ethylene glycol (*11*). Sarcosine and trimethylamine *N*-oxide were shown to induce structure in an early folding intermediate of barstar (*12*). All of these reports indicate that osmolytes mainly change the ensemble of unfolded structures. The increased degree of structure in the unfolded state ensemble should have significant impact on protein stability, explaining why the chemical potential of the unfolded state increases more than that of the folded state in the presence of osmolytes.

Ribosomal protein S6 from *Thermus thermophilus* was envisaged as a good candidate to clarify the effect of osmolytes on the structure of folded and unfolded states. First, it is a small protein (101 amino acid residues) with a two-state folding pathway (*13*). Second, the folding pathway was characterized at the level of specific interactions established by amino acid residues (*14*) and also in the presence of sodium sulfate (*15*) and trehalose (*16*). Third, the unfolded state collapses to a compact, off-folding pathway intermediate in the presence of sodium sulfate (*15*) and trehalose (*16*) showing that the unfolded state ensemble structure might be sensitive to the presence of osmolytes. Sucrose, a disaccharide that accumulates in cyanobacteria under moderate stress conditions, (*1*) was used as a representative candidate of the carbohydrate class of osmolytes, especially because it is commercially available in pure form, free of fluorescent impurities.

MATERIALS AND METHODS

Ribosomal protein S6 from *Thermus thermophilus* was expressed in *E. coli* BL21(DE3)*pLys* and purified as described by Otzen et al. (*13*), except that a Q-sepharose chromatographic step was carried out at pH 8.5 after the CM-sepharose step. S6[11] was eluted from the Q-sepharose column as the first peak with a NaCl gradient, and the purity was >95% as checked by SDS−PAGE. This procedure was applied to wild-type S6 and point mutant LA75 (leucine at position 75 instead of alanine), which was constructed as described by Otzen et al. (*13*). Homogeneity of S6 under folding conditions was checked by HPLC using a gel-filtration column (Bio-Rad Bio-Sil SEC 125-5), and 92% purity was obtained. The remaining 8% were small bumps in the chromatogram, and their presence does not affect the fluorescence lifetimes and amplitudes because S6 yields exactly the same result before and after the gel filtration chromatographic step. S6 has 101 residues (MW 11 973 Da) and a molar extinction coefficient of 12 700 M^{-1} cm^{-1} at 280 nm.

Guanidine hydrochloride (GdnHCl) was obtained from Gibco/BRL Life Technologies (ultrapure), sucrose (>99.5%) and *N*-acetyl-tryptophanamide were obtained from Sigma, and acrylamide (99.9%) was obtained from Bio-Rad. All salts were of analytical grade.

All experiments were performed in 50 mM tris−HCl buffer at pH 8.0 and 25 °C, and S6 was unfolded in the presence of 6 M GdnHCl.

[1] Abbreviations: S6, ribosomal protein S6; F, folded state; U, unfolded state ensemble; ‡, transition state; GdnHCl, guanidinium hydrochloride; NATA, *N*-acetyl-tryptophanamide.

Equilibrium Unfolding Studies. Unfolding of S6 was induced by GdnHCl and measured by fluorescence intensity using excitation at 280 nm and integrating the corrected emission spectra between 300 and 420 nm on a Perkin-Elmer LS-50B fluorescence spectrophotometer with 90° geometry. A rectangular quartz cell with a 10 mm path length was used. Upon S6 unfolding, a decrease on the fluorescence quantum yield and a red shift of the emission maximum were observed (*13*). A final concentration of S6 around 2 μM was used for fluorescence experiments, and for each data point in the unfolding experiment, a stock solution of S6 was diluted into the buffer solution containing the appropriate denaturant concentration. Sucrose was dissolved in both solutions for the assays in the presence of sucrose. Unfolding assessed by far-UV CD was measured on a Jasco J-720 spectropolarimeter using a cylindrical quartz cell with a 1 mm path length and an S6 concentration of around 20 μM. The mean residue ellipticity (deg cm^2 $dmol^{-1}$) at 222 nm was used to monitor the unfolding transition. Two or three replicates were measured for each condition, and average and standard deviation values were calculated.

Stopped-Flow Kinetics. Kinetic experiments were carried out on an Applied Photophysics SX-18MV reaction analyzer (Applied Photophysics, Leatherhead, Surrey, U. K.) with fluorescence-intensity detection. The protein and GdnHCl solutions were mixed in a 1:10 ratio to give a final protein concentration of around 1 μM and the desired denaturant concentration. Whenever sucrose was used, it was present in both solutions. Unfolding was induced by mixing the S6 in buffer with the appropriate GdnHCl solution, and refolding was induced by mixing unfolded S6 in 6.05 M GdnHCl concentration with the appropriate GdnHCl solution. Excitation was always at 280 nm, and the emission was detected above 315 nm using a glass filter.

Steady-State Fluorescence. Fluorescence quantum yields and acrylamide quenching studies were carried out using the Perkin-Elmer LS-50B fluorescence spectrophotometer. A single tryptophan residue of S6 (or *N*-acetyl-tryptophanamide (NATA)) was selectively excited at 296 nm, and emission spectra between 306 and 420 nm were recorded. Absorbance at the excitation wavelength was kept below 0.1 (about 5 μM of S6 was used) to avoid inner filter effects, and emission spectra were corrected by means of a curve obtained with appropriate fluorescence standards (*17*). Refractive indexes used for the calculation of fluorescence quantum yields were taken from published values for sucrose solutions (*18*) and were determined for sucrose plus GdnHCl solutions using an Abbe 60 refractometer (Bellingham & Stanley Limited). Fluorescence quenching studies were carried out by titrating a S6 solution with a stock solution of acrylamide (6 M). The emission intensity was multiplied by a correction factor to account for acrylamide absorbance at the excitation wavelength (*17*). Quenching by acrylamide was related to viscosity values taken from published values for sucrose solutions (*18*) and determined for sucrose plus GdnHCl solutions using a Brookfield digital viscometer (model DV-II) thermostatted with a water bath.

Time-Resolved Fluorescence. Fluorescence decays were obtained for NATA and S6 (at a concentration of about 5 μM) using the time-correlated single photon counting technique (*19*) with a Photon Technology International apparatus (model PTI LS-100), described elsewhere (*20*).

Light from a discharge compartment filled with hydrogen at a relative pressure of −17 in. Hg was collected with the excitation monochromator selected at 296 nm. The instrumental response function (IRF) was obtained using 296 nm scattered light from a Ludox aqueous suspension. Trp fluorescence was collected at 345 nm. Quartz cells of 10 mm were used, and 10^4 photon counts were acquired at the profiles' maxima using 512 channel histograms with 0.163 ns/channel.

Data Analysis. Equilibrium unfolding was fitted to a two-state process according to the following equations

$$y = y_F f_F + y_U f_U \quad (1)$$

$$K_{(U-F)} = \frac{f_U}{f_F} \quad (2)$$

$$\Delta G_{(U-F)} = -RT \ln K_{(U-F)} \quad (3)$$

$$\Delta G_{(U-F)} = \Delta G_{(U-F)}{}^{water} - m_{(U-F)}[\text{GdnHCl}] \quad (4)$$

$$[\text{GdnHCl}]_{50\%} = \frac{\Delta G_{(U-F)}{}^{water}}{m_{(U-F)}} \quad (5)$$

where F and U are folded and unfolded S6, respectively, y is the fluorescence intensity or the mean residue ellipticity at 222 nm, f is the fraction of S6 molecules with a given conformation, K is the equilibrium constant, ΔG is the standard free energy, $m_{(U-F)}$ is the linear dependence of ΔG on GdnHCl concentration, and $[\text{GdnHCl}]_{50\%}$ is the GdnHCl concentration for $\Delta G = 0$. The values for y_F and y_U were calculated directly from pre- and post-transition regions according to the linear dependence.

The effect of sucrose on the global stability of S6 was calculated according to the following equation derived from eqs 4 and 5

$$\Delta\Delta G_{(U-F)}{}^{suc} = \Delta G_{(U-F)}{}^{suc} - \Delta G_{(U-F)}{}^{no\ suc}$$

$$\Delta\Delta G_{(U-F)}{}^{suc} = m_{av}([\text{GdnHCl}]_{50\%}{}^{suc} - [\text{GdnHCl}]_{50\%}{}^{no\ suc}) \quad (6)$$

where suc and no suc refer to the presence or absence of sucrose, respectively, and m_{av} is the average value of $m_{(U-F)}$ for different sucrose concentrations.

In the absence of sucrose, a chevron plot was fitted to a two-state model

$$\log k_{obs} = \log(k_f + k_u) = \log(10^{\log k_f{}^{water} + m_f[\text{GdnHCl}]} + 10^{\log k_u{}^{water} + m_u[\text{GdnHCl}]}) \quad (7)$$

where k_{obs}, k_f and k_u were respectively the observed, the refolding, and the unfolding rate constants and m_f and m_u are constants reflecting the sensitivity to GdnHCl.

In the presence of sucrose, chevron plots were fitted considering a transient intermediate off-folding pathway that equilibrates with the unfolded state within the dead time of the stopped-flow, according to the following scheme: C ↔ U ↔ F (*15*, *21*)

$$\log k_{obs} = \log(f_U k_f + k_u) = \log\left(\frac{k_f}{1 + K_C} + k_u\right)$$

$$\log k_{obs} = \log\left(\frac{10^{\log k_f{}^{water} + m_f[\text{GdnHCl}]}}{1 + 10^{\log K_C{}^{water} + m_C[\text{GdnHCl}]}} + 10^{\log k_u{}^{water} + m_u[\text{GdnHCl}]}\right) \quad (8)$$

where f_U is the fraction of molecules in the unfolded state after equilibration with C, $K_C = [C]/[U]$, and m_C is the constant reflecting the sensitivity of the equilibrium between C and U to GdnHCl.

The effect of sucrose in the stability of C was calculated according to the following equation

$$\Delta\Delta G_{(U-C)}{}^{suc} = \Delta G_{(U-C)}{}^{suc} - \Delta G_{(U-C)}{}^{no\ suc} = 2.303RT(\log K_C{}^{water(suc)} - \log K_C{}^{water(no\ suc)}) \quad (9)$$

where superscript suc indicates the presence of sucrose and no suc, the absence of sucrose.

Fluorescence quantum yields of S6 were calculated relative to NATA at pH 7 ($\Phi_F = 0.13$) with appropriate corrections for the refractive index (*22*)

$$\Phi_F = \Phi_F(\text{NATA})\frac{F}{F_{(NATA)}}\frac{A_{(NATA)}}{A}\frac{n^2}{n^2{}_{(NATA)}} \quad (10)$$

where F is the integrated fluorescence intensity, A is the absorbance at the excitation wavelength, and n is the refractive index.

Fluorescence decays were analyzed using iterative reconvolution of the instrumental response function (IRF) with a single-exponential function for NATA and with a sum of two exponential functions in the case of S6. The Levenberg−Marquardt algorithm (*23*, *24*) implemented in the manufacturer's analysis program and in the designed least-squares routines (*25*) was used to obtain optimal preexponential factors and time constants for each fluorescence decay. The quality of the fits was controlled by means of the usual statistical parameters, χ^2 (0.9−1.2), DW (1.8−2.2), and runs of test Z, as well as by inspection of the distributions of weighted residuals and their autocorrelation functions (*19*).

Intrinsic or natural lifetimes (τ_n) were calculated according to (*22*)

$$\tau_n = \frac{\tau_{av}}{\Phi_F} \quad (11)$$

where τ_{av} is the average lifetime ($\tau_{av} = A_1\tau_1 + A_2\tau_2$) with A being the relative amplitude of each decay time.

Quenching by acrylamide was analyzed using the Stern−Volmer equation (*22*)

$$\frac{F_0}{F} = 1 + K_{SV}[Q] \quad (12)$$

where K_{SV} is the Stern−Volmer constant, including dynamic and static quenching and [Q] is the quencher concentration.

Static quenching usually leads to upward curvatures in Stern−Volmer plots and can be analyzed in terms of the sphere of action within which the probability of quenching

Table 1: Stability Parameters of S6 Wild Type in the Presence of Different Sucrose Concentrations Measured by Steady-State Fluorescence and Far-UV CD[a]

	$\Delta G_{(U-F)}^{water}$ (kcal/mol)	$m_{(U-F)}$ (kcal/mol M)	$[GdnHCl]_{50\%}$ (M)	$\Delta\Delta G_{(U-F)}^{suc}$ (kcal/mol)[b]
fluoresc. int.				
0 M sucrose	8.0 ± 0.7	2.5 ± 0.2	3.15 ± 0.02	
0 M (kinetics)	7.9[c]	2.5[d]	3.15[e]	
0.5 M	11.3 ± 2.0	3.1 ± 0.5	3.64 ± 0.04	1.5
1.0 M	13.8 ± 0.4	3.2 ± 0.0	4.34 ± 0.11	3.7
1.5 M	17.6 ± 6.7	3.4 ± 1.3	5.22 ± 0.22	6.4
1.5 M (kinetics)	13.0[c]	2.5[d]	5.12[e]	4.9[f]
far-UV CD				
0 M sucrose	7.1 ± 2.5	2.2 ± 0.8	3.18 ± 0.04	
0.5 M	8.6 ± 0.9	2.4 ± 0.1	3.63 ± 0.18	1.0
1.0 M	9.5 ± 1.1	2.3 ± 0.2	4.18 ± 0.08	2.3
1.5 M	11.1 ± 1.6	2.1 ± 0.3	5.38 ± 0.08	5.1

[a] All of the values were calculated from equilibrium measurements, except for those referred to as kinetics, which were obtained from stopped-flow measurements. [b] Calculated according to eq 6 with $m_{av} = 3.1 \pm 0.4$ and $m_{av} = 2.3 \pm 0.1$ kcal/(mol M) measured by fluorescence intensity and far-UV CD, respectively. [c] Calculated as $-RT \ln(k_u^{water}/k_f^{water})$. [d] Calculated as $-2.30RT(m_f - m_u)$. [e] GdnHCl concentration, where $k_f = k_u$. [f] Calculated according to eq 6 with $m_{av} = 2.5$ kcal/(mol M) measured by kinetics.

is unity (*22*). A modified form of the Stern−Volmer equation that describes this situation is

$$\frac{F_0}{F} = (1 + K_D[Q])\exp^{(V[Q])} \qquad (13)$$

where V/N_A is the volume of the sphere, N_A is Avogadro's number, and K_D quantifies the dynamic portion of the observed quenching.

If the quenching is known to be only dynamic, then

$$\frac{F_0}{F} = 1 + K_D[Q] = \frac{\tau_0}{\tau} = 1 + k_q\tau_0[Q] \qquad (14)$$

and K_D can be determined by lifetime measurements. The bimolecular quenching constant is given by k_q and τ_0 is the lifetime in the absence of a quencher. The bimolecular quenching constant is linearly related to the sum of the diffusion coefficients of the fluorophore and quencher, which in turn are proportional to the inverse of the viscosity as results from the Stokes−Einstein equation (*22*).

RESULTS

Equilibrium and Kinetics of S6 Unfolding/Refolding in the Presence of Sucrose. The equilibrium stability of ribosomal protein S6 was measured by steady-state fluorescence and far-UV CD in the presence of different sucrose concentrations (Table 1 and Figure 1). The concentrations of GdnHCl at the midpoint are similar using both techniques, within experimental error, showing that the unfolding of secondary and tertiary structures occurs simultaneously in agreement with previous observations in the absence of sucrose (*13*). The large experimental error in the presence of 1.5 M sucrose can be attributed to the high solvent viscosity. Three and two unfolding curves measured by fluorescence and far-UV CD in the presence of 1.5 M sucrose are shown in Figure 1A and B, respectively, to show the variability of data points. Differences between the two techniques were also observed in the cooperativeness of the transition assessed by parameter $m_{(U-F)}$, which is lower on average for CD than that for fluorescence measurements. Errors in $m_{(U-F)}$ lead to large errors in $\Delta G_{(U-F)}^{water}$ (due to large extrapolation) and explain the lower stabilization of S6 by sucrose when measured by

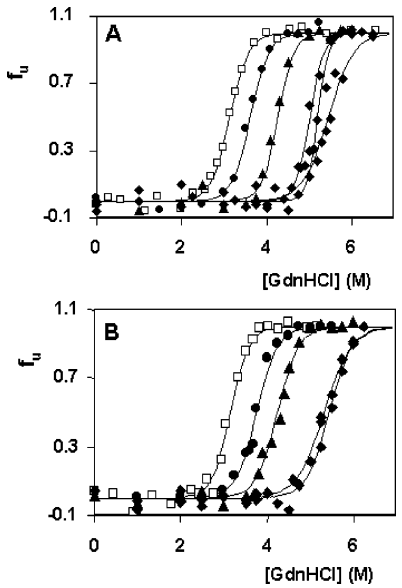

FIGURE 1: Fraction of unfolded S6 (f_U) induced by GdnHCl in the presence of different sucrose concentrations measured by fluorescence intensity (A) and far-UV CD (B). Symbols are for 0 (□), 0.5 (●), 1.0 (▲), and 1.5 M sucrose (◆), and solid lines were calculated from the equation $f_U = e^{(-\Delta G/RT)}/(1 + e^{(-\Delta G/RT)})$ according to a two-state process. Three and two unfolding curves in the presence of 1.5 M sucrose are shown in A and B, respectively, to show the large variability of data when the viscosity is high.

CD ($\Delta\Delta G_{(U-F)}^{suc}$ is lower). Parameter $m_{(U-F)}$ is typically determined with a significantly greater error than that of the midpoint of denaturation because it represents the derivative of the free energy of unfolding with respect to denaturant concentration.

Another test to check the two-state nature of any transition is to examine whether equilibrium and kinetic parameters are identical. Within experimental error, equilibrium and kinetic fluorescence yield the same value of $[GdnHCl]_{50\%}$, the concentration at which 50% of the protein is denatured (Table 1). Again, differences in $\Delta G_{(U-F)}^{water}$, especially in the presence of 1.5 M sucrose, result from small differences in $m_{(U-F)}$ and the large extrapolation from GdnHCl concentrations around the midpoint. Both the similarity between stability parameters measured by fluorescence and CD and those measured by kinetics indicate that equilibrium unfold-

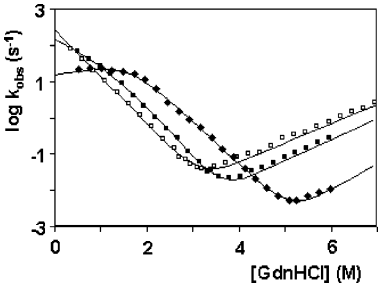

FIGURE 2: Chevron plots of S6 in the absence (□) and presence of 0.75 (■) and 1.5 M sucrose (◆). Solid lines are the fits according to a two-state model in the absence of sucrose (eq 7), considering the accumulation of a compact off-folding pathway intermediate when sucrose is present (eq 8). All fits yielded $R = 0.999$.

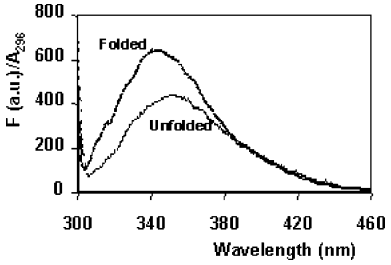

FIGURE 3: Emission spectra of the single tryptophan residues (excitation at 296 nm) of folded and unfolded S6 (6 M GdnHCl) in buffer. Spectra show a decrease in the relative quantum yield and a red shift upon unfolding. Emission maxima were (344 ± 2) and (351 ± 2) nm for folded and unfolded S6, respectively, and showed no significant dependence on sucrose concentration.

ing of S6 in the presence of sucrose is therefore a two-state process in accordance to previous results obtained in water (*13*) and in the presence of trehalose (*16*).

Kinetic measurements often reveal the presence of transient intermediates. Unfolding and refolding kinetics of S6 were found to be single- and double-exponential, respectively, and the chevron plot with the major refolding phase (which accounts for at least 90%) and unfolding phase is shown in Figure 2. In the absence of sucrose, a V-shaped plot was obtained according to the two-state process, as previously shown (*13*). When 0.75 M sucrose is included, the unfolding limb is still linear but the refolding limb shows a slight curvature, suggesting the accumulation of an intermediate with some surface area buried from the solvent (*26*). In the presence of 1.5 M sucrose, although confined to a short concentration range, the unfolding limb also shows a linear dependence on GdnHCl because of the increased stabilization of S6 in sucrose (restricting unfolding measurements to 5−6 M GdnHCl) in combination with the decreased solubility of GdnHCl in sucrose. The refolding limb, however, shows a marked rollover pattern leading to a positive slope at low GdnHCl concentrations. This positive dependence indicates that more denaturant binds to the transition state than to the kinetic ground state, a phenomenon that we attribute to a compact off-pathway intermediate that also accumulates in the presence of sodium sulfate (*15*) and trehalose (*16*). This intermediate is destabilized by GdnHCl because it does not accumulate significantly above 2 M GdnHCl, where the refolding limb shows the expected negative dependence on GdnHCl concentration. Also, it does not accumulate significantly in the transition region and therefore does not affect the two-state nature of the equilibrium unfolding assessed by kinetic measurements. Chevron plots for 0.75 and 1.5 M sucrose were fitted considering the accumulation of this off-pathway intermediate C (data analysis), and the kinetic parameters are shown in Table 2. Sucrose increases the refolding and decreases the unfolding rate constant as expected from the stabilizing effect observed in equilibrium measurements. Sucrose also favors the accumulation of the off-pathway intermediate as revealed by K_C^{water} values (K_C = [C]/[U]). In 0 M GdnHCl with 0.75 M sucrose, 90% of the kinetic ground state is actually C, which equilibrates with the unfolded state within the dead time of the stopped-flow, and this percentage increases to 99% in the presence of 1.5 M sucrose.

Steady-State and Time-Resolved Fluorescence of Folded and Unfolded States of S6. Steady-state fluorescence emissions of the single tryptophan residue of folded S6 and unfolded S6 (in the presence of 6 M GdnHCl) are shown in Figure 3. Unfolding of S6 by GdnHCl decreases the relative quantum yield and shifts the emission peak from 344 to 351 nm. Sucrose does not affect these emission peaks significantly (data not shown). The emission peak of folded S6 reveals a partly exposed Trp residue in limited contact with water (*27*). This agrees with the exposure calculated from the 3D structure of S6 (*28*). The accessible surface area of the tryptophan side-chain residue to water is 67% when compared to the accessible surface area in a Gly-Trp-Gly tripeptide as calculated by Surface Racer (*29*). Figure 4 shows that this exposure results from an indole moiety positioned planar to the surface of the protein in a depression accessible to water (probe radius 1.4 Å). Upon unfolding, the emission peak shifted to 351 nm, characteristic of a fully exposed tryptophan residue (*27*).

Time-resolved tryptophan fluorescence measurements of S6 display two decay times for folded and unfolded S6 despite the single tryptophan residue (Figure 5 and Table 3). For folded S6, 23% of molecules decay with a lifetime of 2.48 ns and the remaining 77% decay with a longer lifetime of 6.43 ns. The two lifetimes decrease to 1.68 and 4.08 ns in the unfolded state of S6, and the relative amplitudes change significantly with the shortest decay

Table 2: Kinetic Parameters for the Unfolding and Refolding of S6 Wild Type in the Absence and Presence of Increasing Concentrations of Sucrose[a]

	k_f^{water} (s^{-1})	m_f (s^{-1} M^{-1})	$k_u^{water} \times 10^5$ (s^{-1})	m_u (s^{-1} M^{-1})	K_C^{water}	m_C (M^{-1})
no sucrose	266 ± 19	−1.30 ± 0.02	45 ± 6	0.53 ± 0.01	[b]	[b]
0.75 M	1597 ± 652	−1.42 ± 0.05	8 ± 2	0.58 ± 0.02	10 ± 3	−0.85 ± 0.13
1.5 M sucrose	2391 ± 428	−1.16 ± 0.02	0.07 ± 0.12	0.70 ± 0.10	157 ± 29	−1.39 ± 0.08

[a] A two-state process was observed in the absence of sucrose (eq 7), and the accumulation of a compact off-folding pathway intermediate (C) occurs in the presence of sucrose (eq 8) according to the scheme C↔U↔F. [b] Data points do not reflect the accumulation of C due to the insufficient dilution of GdnHCl, as accumulation of C seems to occur to some extent even in water (*52*).

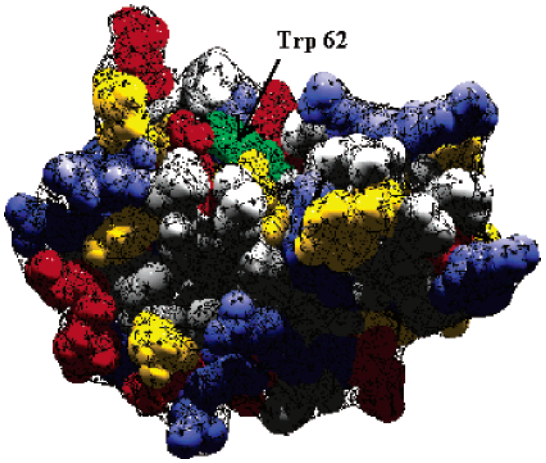

FIGURE 4: Three-dimensional structure of S6 (*28*) showing the van der Waals radii colored according to the characteristics of amino acid residues. Basic amino acids were colored in blue, acidic in red, polar in yellow, and hydrophobic in gray, except for the single Trp residue at position 62, which was colored in green. The molecular surface defined by a water molecule (1.4 Å in size) is shown as a black mesh to highlight the degree of exposure at the molecular surface, especially for Trp 62 (drawn with Swiss-Pdb Viewer (*53*)).

becoming dominant (61%). In fact, the majority of folded proteins with a single tryptophan residue display at least two decay times (*30*−*34*). Despite the proposal of other hypotheses such as the existence of an electron-transfer quenching process (*35*), the major view is that the complexity of the tryptophan fluorescence decay is due to the presence of conformational isomers that are long-lived (millisecond time scale) when compared to the nanosecond time scale of the excited state (*36*, *37*). These isomers are called rotamers because they originate from the rotation of the alanyl side chain of tryptophan (*30*, *22*). The variability of the decays between different proteins seems to be a result of protein structure. The two-decay pattern contrasts to the monoexponential decay of NATA. At pH 7, NATA decays with a 2.6−3.0 ns fluorescence lifetime, regardless of the presence of sucrose or GdnHCl, and these values are similar to the values of 2.9−3.0 ns reported elsewhere (*31*, *38*, *39*). GdnHCl has little or no effect on tryptophan fluorescence (*40*). A single lifetime for NATA is explained by the fact that both groups adjacent to the indole ring are amide functions, and all three rotamers have the carbonyl carbon equidistant from the indole ring (*30*). Because NATA displays a single decay time, the two lifetimes observed for unfolded S6 seem counter-intuitive but are in agreement with previous reports of double-exponential decays for other single-Trp denatured proteins (*31*, *32*). The decay of various proteins denatured in 6 M GdnHCl follow a significantly uniform pattern with a lifetime of around 4 ns and another slightly less than 2 ns as shown for unfolded S6. These results are in contrast with the much larger variation observed for the lifetimes of native proteins and suggest that different proteins assume very similar structures (random coil) in the presence of 6 M GdnHCl.

Lifetimes of folded S6 do not change with the increase in sucrose concentration (Table 3 and Figure 6). In contrast, lifetimes of unfolded S6 clearly show an increasing trend with sucrose concentration. This trend is particularly marked for the longest lifetime, which approaches the value observed for folded S6. Exactly the same behavior was observed for the point mutant of S6 LA75 (leucine at position 75 instead of alanine). This nondisruptive mutation was analyzed here because it was shown previously to stabilize the compact intermediate C favored by trehalose (*16*) and sucrose as shown above. The study of this mutant at different sucrose concentrations might be useful to analyze whether the transient accumulation of C (favored in LA75) results from a structurally different unfolded state (more compact, for instance).

The intrinsic lifetime of the tryptophan residue of S6 is independent of the microenvironment and equals that of NATA (Table 3). Changes in the intrinsic lifetime for single-tryptophan proteins may occur only if a fraction of the protein population or the tryptophan residues is nonfluorescent (*22*). Static quenching of tryptophan fluorescence by buffer components can lead to changes in the intrinsic lifetime, but because no lifetime changes were detected, we can rule out static quenching of both folded and unfolded S6 (unlike the case for acrylamide addition, see below).

Acrylamide Quenching Studies. Collisional quenching of proteins has been extensively used to determine the extent of tryptophan exposure to the aqueous phase (*41*, *42*). First, the quenching of folded S6 was analyzed by steady-state and

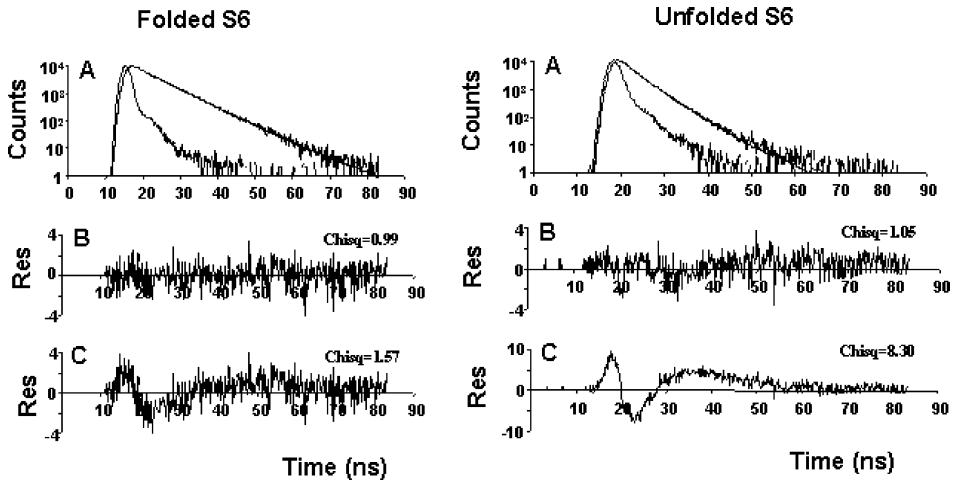

FIGURE 5: Fluorescence-intensity decays of folded S6 (left column) and unfolded S6 in the presence of 6 M GdnHCl (right column) in the absence of sucrose, showing the instrumental response function and a double-exponential fit (A). Parts B and C show the residuals for double- and single-exponential fits, respectively.

Table 3: Lifetimes and Quantum Yields of Fluorescence (Φ_F) for Folded and Unfolded S6 (6 M GdnHCl) in the Presence of Different Sucrose Concentrations[a]

	τ_1 (ns)	A_1	τ_2 (ns)	A_2	Φ_F	τ_n (ns)[b]
NATA (pH 7)						
0 M	2.73				0.14	19.5
0.5 M	2.71				0.13	20.8
1.0 M	2.69				0.16	16.8
1.5 M	2.79				0.16	17.4
2.0 M sucrose	3.03				0.17	17.8
6 M GdnHCl	2.64				0.16	16.5
folded S6						
0 M	2.48 ± 0.20	0.23 ± 0.01	6.43 ± 0.06	0.77 ± 0.01	0.24	23.0
0.5 M	2.50 ± 0.28	0.21 ± 0.03	6.30 ± 0.17	0.79 ± 0.03	0.27	20.4
1.0 M	2.80 ± 0.16	0.24 ± 0.01	6.28 ± 0.09	0.76 ± 0.01	0.24	22.7
1.5 M	2.61 ± 0.40	0.30 ± 0.06	6.19 ± 0.02	0.70 ± 0.06	0.24	21.4
2.0 M sucrose	2.53	0.30	6.13	0.70	0.25	20.2
unfolded S6						
0 M	1.68 ± 0.12	0.61 ± 0.02	4.08 ± 0.10	0.39 ± 0.02	0.11	23.6
0.25M	1.73 ± 0.21	0.60 ± 0.05	4.17 ± 0.19	0.40 ± 0.05	0.13	20.8
0.5 M	1.81 ± 0.02	0.60 ± 0.01	4.32 ± 0.09	0.40 ± 0.01	0.15	18.8
0.75 M	1.81 ± 0.08	0.61 ± 0.04	4.53 ± 0.17	0.39 ± 0.04	0.15	19.1
1.0 M	1.87 ± 0.08	0.58 ± 0.00	4.62 ± 0.06	0.42 ± 0.00	0.16	18.9
1.25 M	2.06 ± 0.04	0.61 ± 0.00	5.06 ± 0.05	0.39 ± 0.00	0.16	20.2
1.5 M sucrose	2.07 ± 0.03	0.59 ± 0.00	5.43 ± 0.13	0.41 ± 0.00	0.15	23.0

[a] *N*-Acetyl-tryptophanamide (NATA) was used as a probe to mimic a completely exposed tryptophan residue. [b] Calculated according to eq 11.

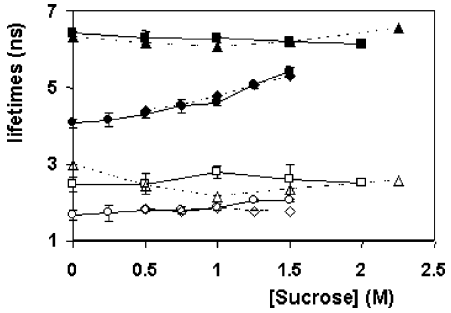

FIGURE 6: Lifetimes of folded and unfolded S6 (6 M GdnHCl) at different sucrose concentrations. The shortest lifetime is shown in empty symbols for wt folded (□), wt unfolded (○), mutant LA75 folded (△), and mutant LA75 unfolded (◇). The longest lifetime is shown in solid symbols for wt folded (■), wt unfolded (●), mutant LA75 folded (▲), and mutant LA75 unfolded (◆). Data points for wt protein and mutant LA75 were connected with solid and dashed lines, respectively, to help with visual inspection.

time-resolved measurements at 23 and 37 °C (Figure 7). The steady-state Stern−Volmer plot at room temperature gave a linear relationship up to an acrylamide concentration of 0.25 M (Figure 7A). However, when high acrylamide concentrations are tested, upward curvatures are observed, indicating that static quenching processes also occur (*43*). Static quenching increases at 37 °C, where an upward curvature is clearly detected below 0.25 M acrylamide. Tryptophan fluorescence of S6 is therefore also quenched by a static mechanism (quencher adjacent to the fluorophore at the moment of excitation resulting in the formation of a nonfluorescent complex), especially at 37 °C. Indeed, the radius of the sphere, where the probability of quenching is 100% is 8.4 Å, is not far from the value of 6−7 Å for the sum of the molecular radii of acrylamide and the indole ring (*44*). The longest lifetime of folded S6 is collisionally quenched by acrylamide, both at 23 and 37 °C (Figure 7B). The lifetime-derived Stern−Volmer constant dependent only on dynamic quenching is very similar at both temperatures (K_D determined from lifetimes is 10.9 and 9.8 M^{-1} at 23 and 37 °C, respectively). The bimolecular quenching constant k_q is larger at 37 °C as

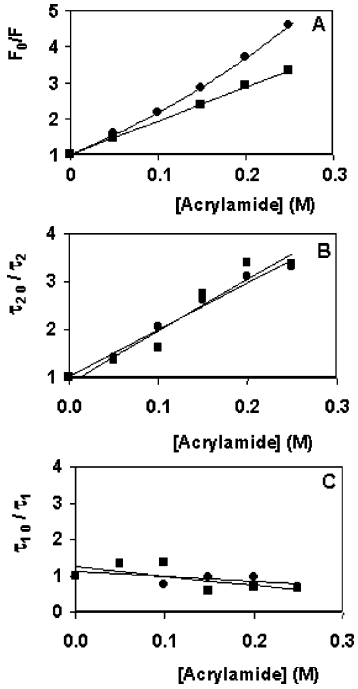

FIGURE 7: Acrylamide quenching of fluorescence from folded S6 at 23 (■) and 37 °C (●). Steady-state fluorescence (A). The straight, solid line at 23 °C is according to eq 12, where $K_{SV} = 9.4$ M^{-1} and $R = 0.99$. The curve at 37 °C is according to eq 13, where $K_D = 8.7$ M^{-1}, $V = 1.47$ M^{-1}, and $R = 0.99$. Time-resolved fluorescence showing the quenching of the longest lifetime (τ_2) (B). Solid lines are according to eq 14, and $R^2 = 0.98$ and $R^2 = 0.93$ at 37 and 23 °C, respectively. Time-resolved fluorescence showing that the shortest lifetime (τ_1) is not quenched by acrylamide (C). Data were fitted to a linear relationship (solid lines) to show that no trend toward increased quenching with acrylamide was observed.

expected (1.7×10^9 and 1.9×10^9 M^{-1} s^{-1} at 23 and 37 °C, respectively) because the lifetime in the absence of acrylamide decreases with the increase in temperature ($k_q = K_D/\tau_0$). The k_q value is linearly related to the sum of the diffusion coefficients of the fluorophore and quencher, and it is expected to increase with the rise in temperature.

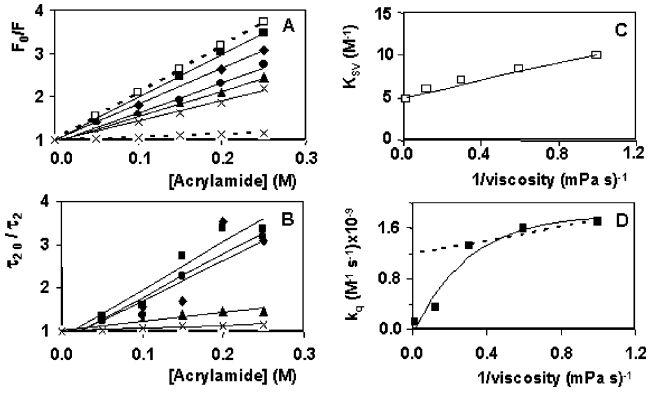

FIGURE 8: Acrylamide quenching of fluorescence from folded S6 at different sucrose concentrations. Steady-state fluorescence emission in the absence of sucrose (■) and the presence of 0.5 (◆), 1.0 (●), 1.5 (▲), and 2.25 M sucrose (×) (A). Solid lines are according to eq 12. Dashed lines were calculated from eq 14 for 0 M (□) and 2.25 M (×) sucrose on the basis of the equality $K_D = k_q\tau_{20}$. Time-resolved fluorescence showing the quenching of the longest lifetime (τ_2) (B). Data points indicate the absence of sucrose (■) and presence of 0.5 (◆), 1.0 (●), 1.5 (▲), and 2.25 M sucrose (×). Data points were used to linearly fit the data and calculate k_q (solid lines according to eq 14). Linear relationship between the Stern−Volmer quenching constant K_{SV} (calculated from A) and the inverse of viscosity ($R^2 = 0.98$) (C). The bimolecular quenching constant k_q for τ_2 (calculated from the linear fits shown in B) is directly proportional to 1/viscosity at low viscosity values (up to around 3.5 mPa s) as shown by the dashed line ($R^2 = 0.89$) (D). At higher viscosity values (high sucrose concentrations) k_q decreases more than anticipated by the increase in viscosity as clearly shown by the solid line.

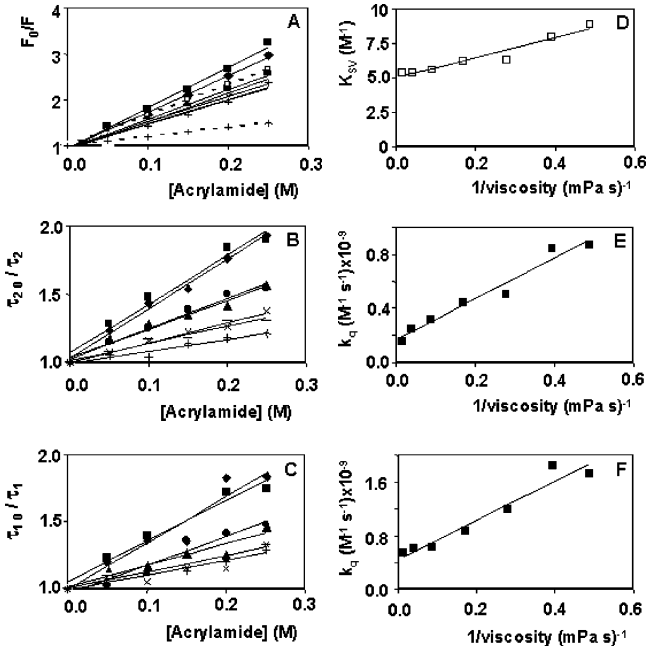

FIGURE 9: Acrylamide quenching of fluorescence from unfolded S6 (6 M GdnHCl) at different sucrose concentrations: absence of sucrose (■) and presence of 0.25 (◆), 0.5 (●), 0.75 (▲), 1.0 (×), 1.25 (−), and 1.5 M sucrose (+). Steady-state fluorescence emission (A). Solid lines are according to eq 12. Dashed lines were calculated from eq 14 for 0 (□) and 1.5 M (+) sucrose on the basis of the equality $K_D = k_{q1}\tau_{10} + k_{q2}\tau_{20}$. Time-resolved fluorescence showing the quenching of the longest lifetime (τ_2) (B). Solid lines are according to eq 14. Time-resolved fluorescence showing the quenching of the shortest lifetime (τ_1) (C). Solid lines are according to eq 14. Linear relationship between the Stern−Volmer quenching constant K_{SV} (calculated from the linear fits shown in A) and the inverse of viscosity ($R^2 = 0.94$) (D). Linear relationship between the bimolecular quenching constant k_q for τ_2 (calculated from the linear fits shown in B) and the inverse of viscosity ($R^2 = 0.97$) (E). Linear relationship between the bimolecular quenching constant k_q for τ_1 (calculated from the linear fits shown in C) and the inverse of viscosity ($R^2 = 0.94$) (F).

No significant collisional quenching by acrylamide was observed for the shortest lifetime of folded S6 at both temperatures (Figure 7C). Significantly different degrees of collisional quenching were observed for different lifetime components of other single Trp residue proteins (*34*). An unfavorable orientation of the species emitting with the shortest lifetime should not be the reason for this observation, as the quenching reaction does not seem to have stereochemical requirements (*41*). However, the lack of accessibility of the tryptophan rotamer to acrylamide (*34*) might explain the absence of collisional quenching. Tryptophan residues may show little or no motion at the subnanosecond time scale, even when exposed to the aqueous phase (*30*). It should be made absolutely clear that the macroheterogeneity of S6 in the folded state (more than one stable conformation), which could be another reason for the inacessibility of the shortest lifetime to acrylamide, does not occur as shown by gel filtration HPLC chromatography (Materials and Methods). Comparison between acrylamide quenching studies carried out at 23 and 37 °C were very important in forming conclusions regarding the quenching pattern of folded S6. At 23 °C, τ_2 approaches τ_1 with an increase in acrylamide concentration, and the double-exponential nature of the decay becomes more difficult to assign. At 37 °C, τ_2 is more quenched by acrylamide and becomes even shorter than τ_1 at high acrylamide concentrations. Fluorescence quenching studies at 37 °C were carried out to confirm and identify the collisional quenching of τ_2 and the collisionally unquenched state of τ_1 more clearly.

Quenching of folded S6 by acrylamide decreases with an increase in sucrose concentration (Figure 8A and B). Collisonal quenching of τ_2 as assessed by the bimolecular quenching constant k_q was calculated from the slope of the linear part of Figure 8B and plotted against the inverse of viscosity (Figure 8D). The k_q value is directly proportional to the diffusion coefficient of the quencher, and the latter is inversely proportional to the viscosity of the solvent, according to the Stokes−Einstein equation (*22*). Decreased collisional quenching with the increase in sucrose concentration up to 1 M is explained by the effect of sucrose on the viscosity of the solvent. Above 1 M sucrose (corresponding to the two data points with lowest 1/viscosity values in Figure 8D), k_q decreases more than predicted by the increase in viscosity, indicating that tryptophan exposure to acrylamide decreases in the presence of high sucrose concentrations. This additional decrease in k_q is not reflected in K_{SV} because static quenching becomes significant at high sucrose concentrations (Figure 8C). This conclusion is quantitatively supported by a comparison of K_{SV} and K_D values. At 0 M sucrose, K_{SV} is 9.4 M^{-1} and K_D is 10.9 M^{-1}, and at 2.25 M sucrose, K_{SV} is 4.7 M^{-1} and K_D is 0.6 M^{-1} (7.8-fold decrease).

Unfolded S6 in the presence of 6 M GdnHCl is close to a random coil structure, and both rotamers emitting with the longest and the shortest lifetimes are accessible and collisionally quenched by acrylamide (Figure 9B and C). Collisional quenching of τ_1 and τ_2 at different sucrose concentrations was again evaluated by using the bimolecular quenching constant. Decreased k_q values for τ_1 and τ_2 with

an increase in sucrose concentration are completely explained by the effect of sucrose on the viscosity of the solvent (Figure 9E and F). Contrary to the folded state, tryptophan exposure to acrylamide in the unfolded state does not decrease in the presence of high concentrations of sucrose. Interestingly, k_q values for τ_1 are larger than those measured for τ_2. This is probably due to the differential accessibility to acrylamide of different rotamers, even for structures close to random coils (*34*). Quenching of NATA fluorescence by acrylamide in 6.7 M GdnHCl has a k_q value (3.4×10^9 M^{-1} s^{-1} (*44*)) larger than those of unfolded S6, indicating some shielding of the tryptophan residue from acrylamide. A growing number of studies indicate that the unfolded state forms transient structures with relaxation times in the μs range (*45*). Values of K_{SV} for unfolded S6 show a linear relationship with the inverse of viscosity, reflecting the decrease in k_q for the two lifetimes (Figure 9D).

DISCUSSION

Sucrose Shifts the Two-State Unfolding of S6 toward the Folded State. The presence of sucrose increases the stability of S6 by a factor of 3.8 ± 0.7 kcal/mol/M of sucrose, as seen by averaging fluorescence and CD data (Table 1). This value is not far from the stabilizing effect of trehalose (3.0 ± 0.1 kcal/mol/M) (*16*). S6 unfolds according to a two-state process under equilibrium conditions (*13*), and sucrose does not change this two-state nature. No stable intermediates were found to accumulate within the transition region because the unfolding of secondary and tertiary structures occur simultaneously, and the stability parameters of S6 determined from equilibrium and kinetic measurements are coincident within experimental error (Table 1 and Figure 1).

Kinetics of Refolding Show That Sucrose Favors the Transient Compaction of Unfolded S6 Under Native Conditions. The kinetics of refolding of S6 reveal that sucrose stabilizes a compact intermediate C that accumulates off the folding pathway (Table 2). This intermediate, which accumulates transiently at low GdnHCl concentrations, was first detected in the presence of sodium sulfate (*15*). It equilibrates with the unfolded state during the dead time of the stopped flow and is more compact (less surface area exposed to solvent) than the transition state for folding. The overall conversion of this compact state to the transition state for folding is globally an unfolding process and therefore is characterized by a positive dependence on GdnHCl concentration (Figure 2). Comparing the stabilization of the folded state and C by 1 M sucrose (comparing the values of $\Delta\Delta G_{(U-F)}^{suc}$ and $\Delta\Delta G_{(U-C)}^{suc}$ measured by fluorescence), it can be concluded that C is stabilized 51% as much as that of the folded state. Recently, trehalose was shown to stabilize significantly this intermediate that contains non-native diffuse contacts (*16*). In the presence of 1 M trehalose, C is stabilized 90% as much as that of the folded state of S6. Interestingly, trehalose induces the same effect of collapsing the unfolded ensemble to an off-pathway intermediate on the larger (22.5 KDa) enzyme cutinase (*46*). All of these data show that osmolytes, namely, trehalose and sucrose, induce a fast collapse of the unfolded ensemble to a compact species when this ensemble is suddenly placed under native conditions. In contrast, the linear relationship observed in the chevron plot unfolding limb of S6 is not affected by the presence of sucrose, and S6 unfolding measured by kinetics proceeds according to a two-state process (Table 2 and Figure 2). Exactly the same was observed for S6 in the presence of trehalose (*16*). Even for cutinase, where an on-unfolding pathway intermediate was observed, trehalose does not change the pattern of the unfolding limb, that is, the characteristics of the unfolding pathway (*46*). Clearly, no intermediates were detected during the kinetic unfolding of S6 in the presence of sucrose showing that the folded state of S6 in the presence of sucrose does not equilibrate with any intermediate under denaturing conditions.

Fluorescence Lifetimes Reveal No Significant Conformational Changes of Folded and Unfolded S6 in the Presence of Sucrose. Steady-state and time-resolved fluorescence were used to probe the structure of S6 in the folded and unfolded states in the presence of increasing amounts of sucrose. Time-resolved fluorescence, in particular, is a high-resolution technique with extreme sensitivity to protein conformational changes. Both folded and unfolded S6 display two lifetimes, despite the presence of a single tryptophan residue (Table 3 and Figure 5). Several other proteins with a single tryptophan residue display two decay times due to the existence of different rotamers (*30*−*32*). Variability of the decays for the folded state of proteins is a result of different protein structures. Increasing sucrose concentration has no effect on the lifetimes of folded S6, indicating no significant conformational changes of S6 in the presence of sucrose (Figure 6). The lifetime of the single tryptophan residue of a phosphocarrier protein was shown to decrease slightly in the presence of sucrose, but this effect was due to the increase in the refractive index induced by sucrose (*47*). Unfolded S6 in 6 M GdnHCl also shows two decay times that are shorter than the ones observed for folded S6 and are very similar to lifetimes reported for other denatured proteins (*31*, *32*). Proteins unfolded by high concentrations of GdnHCl seem to have a rather uniform pattern of fluorescence decay, reflecting a common structure close to a random coil. Quantitative differences in the decay parameters observed for denatured proteins, which are apparently in their random coil state, may be attributed to differences in the local structure (*32*).

Lifetimes of unfolded S6 increase with the increase in sucrose concentration, approaching the values observed for folded S6 (Figure 6). This trend is particularly evident for the longest lifetime. Apparently, this would indicate that sucrose induces a conformational change in the unfolded state of S6 that might become more compact (increased lifetimes) with the increase in sucrose concentration. However, the single tryptophan residue of S6 for a random coil structure is fully exposed to the solvent (Figure 3), and contrary to the folded state, where lifetimes are highly dependent on the nature of side chains in close proximity to the indole moiety, lifetimes for a fully exposed tryptophan residue are dependent mostly on quenching by solvent molecules. Sucrose increases the viscosity of the solvent very significantly, leading to a decrease in collisional quenching by solvent molecules. The increase in solvent viscosity can thus lead to increased lifetimes for unfolded S6. This effect does not occur significantly for the folded state of S6 because quenching processes for a partly exposed tryptophan residue are mostly dependent on neighboring side chains. This point of view is supported by three other observations. First, the longest lifetime of unfolded S6 increases more significantly than the shortest one because the degree of collisional

quenching is proportional to the lifetime. Second, the S6 mutant LA75 shows exactly the same pattern and magnitude for the increase in lifetimes as the wild type protein (Figure 6). If increased lifetimes result from increased compaction of unfolded S6, then lifetimes may increase more significantly for LA75 as this mutation favors the transient collapse of the unfolded state to C (*16*). Third, collisional quenching by acrylamide of unfolded S6 is fully explained by the increase in solvent viscosity induced by sucrose (Figure 9).

Acrylamide Quenching Studies Show That Sucrose at High Concentrations Induces the Compaction of Folded S6. The three points described above indicate that up to 1.5 M concentration of sucrose has no effect on the compaction/conformation of the unfolded state induced by 6 M GdnHCl, which is close to a random coil with two lifetimes accessible to collisions with acrylamide (Figure 9B and C). Decreased collisional quenching by acrylamide in the presence of sucrose is exclusively due to the increased viscosity and not to the decreased accessibility of the tryptophan residue (Figure 9E and F). This is in clear contrast to the effect of sucrose on the accessibility of the tryptophan residue in the folded state of S6. The longest lifetime of folded S6 is collisionally quenched by acrylamide, and up to 1 M concentration of sucrose decreases the rate of collisions because it increases the viscosity of the solvent (Figure 8B and D). However, above 1 M sucrose, the decrease in the collisional rate of acrylamide is much larger than that predicted by the increase in viscosity. The most logical and plausible explanation is that accessibility of the tryptophan residue to the solvent above 1 M sucrose has decreased as a result of increased compaction of the folded state. Decreased accessibility to collisions with acrylamide cannot be explained by a shift in the equilibrium toward the nonaccessible tryptophan rotamer. This shift will formally affect the amplitude of each lifetime but not the lifetime itself. Decreased accessibility at high sucrose concentrations might be related to the microenvironment of the Trp residue, which is 67% solvent-exposed and therefore provides a uniquely sensitive probe of conformational changes. Small conformational changes around the Trp ring caused by sucrose may be sufficient to increase its degree of burial and consequently lower its accessibility to acrylamide. Tightening of the native structure of azurin in the presence of 2 M sucrose was shown also to occur on the basis of phosphorescence lifetimes and acrylamide quenching studies (*48*). Decreased accessibility of the tryptophan residue of S6 is not associated to large conformational changes, as the lifetimes of folded S6 do not change in the presence of sucrose (Table 3 and Figure 6). This explanation seems to be supported by kinetic data. If the folded state becomes more compact above 1 M sucrose, this should lead to an increased m_u value: the constant reflecting the sensitivity of unfolding to GdnHCl, which is proportional to the degree of residue exposure occurring in the conversion from the folded to the transition state (*26*). Indeed, m_u increases in the presence of 1.5 M sucrose although displaying a large error due to a low number of data points used to fit the data (Table 2 and Figure 2). Unfortunately, unfolding kinetics in the presence of higher sucrose concentrations are experimentally inaccessible because of the decreased solubility of GdnHCl in sucrose; otherwise, a further increase in m_u would certainly be detected.

Compaction of S6 Induced by Sucrose Is Counterbalanced by the Denaturing Effect of GdnHCl and Therefore Is Observed Only Under Native Conditions. Osmolytes, such as sucrose and trehalose, are known to stabilize the folded state of proteins (or destabilize the unfolded state) in contrast to the effect of urea or GdnHCl, which are the most widely used protein denaturants. They have opposite effects on the stability of proteins, and the presence of one counteracts the effect of the other. The unfolded state of S6 in the presence of 1.5 M sucrose is totally converted to a highly compact structure. The high degree of compactness of this intermediate (75% as compact as the folded state as calculated from $m_C/(m_f - m_u)$) favored by sucrose reflects the wide conformational space available to the unfolded state. When the unfolded state in the presence of sucrose is suddenly placed under native conditions during the stopped-flow experiment, it has a wide range of conformational space available to increase its compactness. The presence of 6 M GdnHCl counteracts the effect of sucrose, and no compaction of the unfolded state is detected as probed by the accessibility of the tryptophan residue to collisions with acrylamide. Other pairs of osmolyte-denaturants such as the urea-trimethylamine *N*-oxide also show counteraction effects on Rnase A structural fluctuations (*49*). The folded state of S6 has a much narrower range of conformational space available to become more compact. However, in the presence of high sucrose concentrations ($\geq$1.5 M sucrose) with no GdnHCl to counteract sucrose's effect, decreased accessibility of the tryptophan residue to collisions with acrylamide indicates an increased compaction of the folded S6 state. Increased compactness or structure acquisition induced by osmolytes both for folded (*48*, *49*) and unfolded states (*10*−*12*, *50*) was reported for other proteins and suggested to be the mechanism by which osmolytes increase protein stability (*16*, *51*). Compactness of protein conformational states induced by osmolytes seem, however, to be significantly stronger for less-packed polypeptides (*48*), explaining 75% of the compactness observed for unfolded S6 under native conditions. Regarding protein stability, decreased conformational entropy, especially of the unfolded ensemble with increased compactness but without native contacts, favors the folded state by destabilizing the unfolded state. Decreased conformational entropy of the folded state in the presence of osmolytes might be, at least partly, compensated by an enthalphic contribution from native interactions that strengthen under compaction.

ACKNOWLEDGMENT

We acknowledge Professor João Pessoa from Instituto Superior Técnico for the use of the CD facilities.

REFERENCES

1. Brown, A. D. (1990) Compatible solutes in *Microbial water stress physiology: Principles and Perspectives*, pp 241−275, John Wiley and Sons, New York.
2. Hincha, D. K., and Hagemann, M. (2004) Stabilization of model membranes during drying by compatible solutes involved in the stress tolerance of plants and microorganisms, *Biochem. J. 383*, 277−283.
3. Timasheff, S. N. (1995) Solvent stabilization of protein structure in *Protein Stability and Folding: Theory and Practice* (Shirley, B. A., Ed.), pp 253−269, Humana Press, Totowa, NJ.
4. Xie, G., and Timasheff, S. N. (1997) The thermodynamic mechanism of protein stabilization by trehalose, *Biophys. Chem. 64*, 25−43.

5. Xie, G., and Timasheff S. N. (1997) Temperature dependence of the preferential interactions of ribonuclease A in aqueous cosolvent systems: Thermodynamic analysis, *Protein Sci. 6*, 222−232.
6. Liu, Y., and Bolen, D. W. (1995) The peptide backbone plays a dominant role in protein stabilization by naturally occurring osmolytes, *Biochemistry 34*, 12884−12891.
7. Wang, A., and Bolen, D. W. (1997) A naturally occurring protective system in urea-rich cells: Mechanism of osmolyte protection of proteins against urea denaturation, *Biochemistry 36*, 9101−9108.
8. Bolen, D. W., and Baskakov, I. V. (2001) The osmophobic effect: Natural selection of a thermodynamic force in protein folding, *J. Mol. Biol. 310*, 955−963.
9. Sánchez, I. E., and Kiefhaber, T. (2003) Hammond behavior *versus* ground-state effects in protein folding: Evidence for narrow free energy barriers and residual structure in unfolded states, *J. Mol. Biol. 327*, 867−884.
10. Qu, Y., Bolen, C. L., and Bolen, D. W. (1998) Osmolyte-driven contraction of a random coil protein, *Proc. Natl. Acad. Sci. U.S.A. 95*, 9268−9273.
11. Silow, M., and Oliveberg, M. (2003) High concentrations of viscogens decrease the protein folding rate constant by prematurely collapsing the coil, *J. Mol. Biol. 326*, 263−271.
12. Pradeep, L., and Udgaonkar, J. B. (2004) Osmolytes induce structure in an early intermediate on the folding pathway of barstar, *J. Biol. Chem. 279*, 40303−40313.
13. Otzen, D. E., Kristensen O., Proctor, M., and Oliveberg, M. (1999) Structural changes in the transition state of protein folding: Alternative interpretations of curved chevron plots, *Biochemistry 38*, 6499−6511.
14. Otzen, D. E., and Oliveberg, M. (2002) Conformational plasticity in folding of the split β-α-β protein S6: Evidence for burst-phase disruption of the native state, *J. Mol. Biol. 317*, 613−627.
15. Otzen, D. E., and Oliveberg, M. (1999) Salt-induced detour through compact regions of the protein folding landscape, *Proc. Natl. Acad. Sci. U.S.A. 96*, 11746−11751.
16. Chen, L. Y., Cabrita, G. J. M., Otzen, D. E., and Melo, E. P. (2005) Stabilization of the ribosomal protein S6 by trehalose is counterbalanced by the formation of a putative off-pathway species, *J. Mol. Biol. 351*, 402−416.
17. Andrade, S. M., and Costa, S. M. B. (2002) Spectroscopic studies on the interaction of a water soluble porphyrin and two drug carrier proteins, *Biophys. J. 82*, 1607−1619.
18. Lide, D. R. (1999) *Handbook of Chemistry and Physics*, CRC Press, New York.
19. O'Connor, D. V., and Philips, D. (1984) *Time-Correlated Single Photon Counting*, Academic Press, New York.
20. Medeiros, G. M. M., Leitão, M. F., and Costa, S. M. B. (1993) Fluorescence of acridine and acridine 9-carboxylic acid in anionic micelles, *J. Photochem. Photobiol., A 72*, 225−233.
21. Otzen, D. E. (2005) Expansion during folding of a collapsed state, *Biochim. Biophys. Acta 1750*, 146−153.
22. Lakowicz, J. R. (1999) *Principles of Fluorescence Spectroscopy*, Kluwer Academic /Plenum Publishers, New York.
23. Levenberg, K. (1944) A method for the solution of certain non-linear problems in least squares, *Q. Appl. Math. 2*, 164−168.
24. Marquardt, D. (1963) An algorithm for least-squares estimation of non-linear parameters, *SIAM J. Appl. Math. 11*, 431−441.
25. Ferreira, J. A. B., Coutinho, P. J. G., Costa, S. M. B., and Martinho, J. M. G. (2000) Transient photokinetics of Rhodamine 3B+ClO4- in water: toluene mixtures, *Chem. Phys. 262*, 453−465.
26. Fersht, A. (1999) *Structure and Mechanism in Protein Science*, W. H. Freeman and Company, New York.
27. Burstein, E. A., Vedenkina, N. S., and Ivkova, M. N. (1973) Fluorescence and the location of tryptophan residues in protein molecules, *Photochem. Photobiol. 18*, 263−279.
28. Lindahl, M., Svensson, L. A., Liljas, A., Sedelnikova, S. E., Eliseikina, I. A., Fomenkova, N. P., Nevskaya, N., Nikonov, S. V., Garber, M. B., Muranova, T. A., Rykonova, A. I., and Amons, R. (1994) Crystal structure of the ribossomal protein S6 from *Thermus thermophilus*, *EMBO J. 13*, 1249−1254.
29. Tsodikov, O. V., Record, M. T., Jr., and Sergeev, Y. V. (2002) A novel computer program for fast exact calculation of accessible and molecular surface areas and average surface curvature, *J. Comput. Chem. 23*, 600−609.
30. Beechem, J. M., and Brand, L. (1985) Time-resolved fluorescence of proteins, *Annu. Rev. Biochem. 54*, 43−71.
31. Grinvald, A., and Steinberg, I. Z. (1976) The fluorescence decay of tryptophan residues in native and denaturated proteins, *Biochim. Biophys. Acta 427*, 663−678.
32. Swaminathan, R., Krishnamoorthy, G., and Periasamy, N. (1994) Similarity of fluorescence lifetime distribution for single tryptophan proteins in the random coil state, *Biophys. J. 67*, 2013−2023.
33. Soulages, J. L., and Arrese, E. L. (2000) Fluorescence spectroscopy of single tryptophan mutants of Apolipophorin-III in discoidal lipoproteins of dimyristoylphosphatidylcholine, *Biochemistry 39*, 10574−10580.
34. Hellings, M., De Maeyer, M., Verheyden, S., Hao, Q., Van Damme, E. J. M., Peumans, W. J., and Engelborghs, Y. (2003) The dead-end elimination method, tryptophan rotamers and fluorescence lifetimes, *Biophys. J. 85*, 1894−1902.
35. Liu, T., Callis, P. R., Hesp, B. H., de Groot, M., Buma, W. J., and Broos, J. (2005) Ionization potentials of fluoroindoles and the origin of nonexponential tryptophan fluorescence decay in proteins, *J. Am. Chem. Soc. 127*, 4104−4113.
36. Ross, J. B. A., Wyssbrod, H. R., Porter, R. A., Schwartz, G. P., Michaels, C. A., and Laws, W. R. (1992) Correlation of tryptophan fluorescence-intensity decay parameters with ^{1}H NMR-determined rotamer conformations: [tryptophan^2]oxytocin, *Biochemistry 31*, 1585−1594.
37. Dahms, T. E. S., Willis, K. J., and Szabo, A. G. (1995) Conformational heterogeneity of tryptophan in a protein crystal, *J. Am. Chem. Soc. 117*, 2321−2326.
38. Eftink, M. R., Jia, Y., Hu, D., Ghiron, C. A. (1995) Fluorescence studies with tryptophan analogues: Excited-state interactions involving the side chain amino group, *J. Phys. Chem. 99*, 5713−5723.
39. Szabo, A. G., and Rayner, D. M. (1980) Fluorescence decay of tryptophan conformers in aqueous solution, *J. Am. Chem. Soc. 102*, 554−563.
40. Kronman, M. J., and Holmes, L. G. (1971) The fluorescence of native, denaturated and reduced-denaturated proteins, *Photochem. Photobiol. 14*, 113−134.
41. Eftink, M. R., and Ghiron, C. A. (1976) Exposure of tryptophanyl residues in proteins. Quantitative determinations by fluorescence quenching studies, *Biochemistry 15*, 672−680.
42. Eftink, M. R., and Ghiron, C. A. (1981) Fluorescence quenching studies with proteins, *Anal. Biochem. 114*, 199−227.
43. Pedersen, J. S., Christensen, G., and Otzen, D. E. (2004) Modulation of S6 fibrillation by unfolding rates and gatekeeper residues, *J. Mol. Biol. 341*, 575−588.
44. Eftink, M. R., and Ghiron, C. A. (1976) Fluorescence quenching of indole and model micelle systems, *J. Phys. Chem. 80*, 486−493.
45. Chattopadhyay, K., Elson, E. L., and Frieden, C. (2005) The kinetics of conformational fluctuations in an unfolded protein measured by fluorescence methods, *Proc. Natl. Acad. Sci. U.S.A. 102*, 2385−2389.
46. Melo, E. P., Chen, L.-Y., Cabral, J. M. S., Fojan, P., Petersen, S. B., and Otzen, D. E. (2003) Trehalose favors a cutinase compact intermediate off-folding pathway, *Biochemistry 42*, 7611−7617.
47. Toptygin, D., Savtchenko, R. S., Meadow, N. D., Roseman, S., and Brand, L. (2002) Effect of the solvent refractive index on the excited-state lifetime of a single tryptophan residue in a protein, *J. Phys. Chem. B 106*, 3724−3734.
48. Cioni, P., Bramanti, E., and Strambini, G. B. (2005) Effects of sucrose on the internal dynamics of azurin, *Biophys. J. 88*, 4213−4222.
49. Qu, Y., and Bolen, D. W. (2003) Hydrogen exchange kinetics of Rnase A and the urea:TMAO paradigm, *Biochemistry 42*, 5837−5849.
50. Minton, A. P. (2005) Models for excluded volume interaction between an unfolded protein and rigid macromolecular cosolutes: Macromolecular crowding and protein stability revisited, *Biophys. J. 88*, 971−985.
51. Cheung, M. S., Klimov, D., and Thirumalai, D. (2005) Molecular crowding enhances native state stability and refolding rates of globular proteins, *Proc. Natl. Acad. Sci. U.S.A. 102*, 4753−4758.
52. Otzen, D. E., and Oliveberg, M. (2001) A simple way to measure protein refolding rates in water, *J. Mol. Biol. 313*, 479−483.
53. Guex, N., and Peitsch, M. C. (1997) SWISS-MODEL and the Swiss-Pdb Viewer: An environment for comparative protein modeling, *Electrophoresis 18*, 2714−2723.

BI051490G